Molecular Motions in Crystalline Anthracene and Naphthalene from Multitemperature Diffraction Data

by **Hans-Beat Bürgi***, **Narayanan Rangavittal**, and **Jürg Hauser**

Laboratorium für Kristallographie, Universität Bern, Freiestrasse 3, CH-3012 Bern
(phone +41 31 631 42 82; fax +41 31 631 39 96; e-mail: hans-beat.buergi@krist.unibe.ch)

Dedicated to *Edgar Heilbronner*, in admination

Atomic Displacement Parameters (ADPs) of anthracene (94–295 K), (D_{10})anthracene (16, 295 K), naphthalene (92–239 K), and (D_8)naphthalene (12, 295 K) have been analyzed with the help of an *Einstein*-type model of local, molecular normal modes. The low-frequency motions are expressed in terms of molecular translations, librations, and deformations, and account for the temperature dependence of the experimental ADPs. Their frequencies decrease with increasing temperature due to crystal expansion. For anthracene, enough data of sufficient quality are available to determine two low-frequency out-of-plane deformation modes. The corresponding frequencies of naphthalene are much higher and cannot be extracted from the available data, which are more limited qualitatively and quantitatively. The mean-square amplitudes due to the high-frequency normal modes are also extracted from the diffraction data. They agree satisfactorily with those obtained for molecules in the gas phase from density-functional theory. Contributions to the ADPs that cannot be interpreted in terms of motion are small but significant. The case study presented here shows that dynamic aspects of molecular structure can be obtained from single-crystal diffraction studies. For optimal results, experiments must be performed over as large a temperature and resolution range as possible, and factors affecting ADP's but not representing motion have to be kept to a minimum, *e.g.*, by avoiding disorder, parametrizing X-ray data with multipole models, and minimizing absorption and extinction.

Introduction. – Single-crystal diffraction experiments are generally seen as providing a static picture of crystal structure. They are certainly not considered the method of choice for studying the dynamics of molecules in the solid state, although atomic-displacement parameters (ADPs) – or temperature-factor parameters, or vibrational parameters, as they are variously called – are determined routinely in every crystal-structure analysis. There are several reasons for this state of affairs: *1*) ADPs are *mean-square displacements*, implying that their phases, *i.e.*, their signs, are lost. This makes it difficult to study collective motions of atoms in molecules and unit-cells. *2*) Diffraction measurements are affected by many kinds of factors related to crystal quality whose importance is difficult to assess (systematic errors). This has led to widely differing opinions among crystallographers and patrons of crystal structures about the physical significance of ADPs. Are they quantitative measures of motion and minor positional disorder, or convenient parameters to improve least-squares agreement or, more likely, something in between? *3*) The mean-square amplitudes are given as a 3×3, symmetric matrices whose relevance is more difficult to grasp than that of simple bond distances and angles. Some qualitative information can usually be gleaned from graphical representations such as ORTEP or PEANUT plots, the former displaying ellipsoids of constant probability of finding an atom, the latter representing the (root-)

mean-square displacement in all directions of space [1][2]. Needless to say that, however suggestive such plots may be, their visual interpretation must remain tentative at best.

Anthracene, naphthalene, and benzene have played a central role in attempts to unravel the information encoded in the ADPs. As early as 1956, *Cruickshank* determined anisotropic ADPs of anthracene and developed a method to derive amplitudes of molecular translation and libration from them [3][4]. His method assumes that the molecule is essentially rigid, and that the intramolecular amplitudes are negligible, thus getting the phase problem out of the way. Analysis of ADPs has become more widely used after *Schomaker* and *Trueblood*'s definitive mathematical formulation of the rigid-body model [5]. Effects of intramolecular vibrations are usually not considered in such studies except for the light H- and D-atoms. Their zero-point amplitudes are significant and can be estimated relatively easily from spectroscopic stretching and bending frequencies [6].

The proportion of the ADPs due to motion can be assessed from their temperature dependence. It was again *Cruickshank* who pioneered this idea by predicting the variation of translation and libration amplitudes with temperature [7]. His ideas were tested in three studies by *Brock*, *Dunitz*, and *Hirshfeld* (see *Experimental*). The first two report on rigid-body analyses of ADPs determined for anthracene between 94 and 295 K [8], and for naphthalene between 92 and 239 K [9]. In the third paper, new libration and translation amplitudes are reported based on a re-analysis of the diffraction data with better atomic scattering factors (multipole refinements) [10]. All analyses were done separately for each temperature. To compare the results obtained at different temperatures, harmonic-oscillator frequencies were obtained *a posteriori* from the translation and libration amplitudes, respectively. Their temperature dependence as well as that of the translation and libration amplitudes was found to agree qualitatively with *Cruickshank*'s prediction. After discussing various sources of error in the experimental data, comparing their results with spectroscopic data and lattice dynamical force-field models, the authors conclude that they '*do not know the true values of the ADPs and the lattice dynamical values may not be too reliable a guide*' [10].

A major limitations of such studies has probably been the lack of an internally consistent model expressing ADPs over a large range of temperatures in terms of a single set of physically meaningful parameters. Such a model must *1*) account for temperature-dependent and -independent components of ADPs as well as for softening of the crystal field due to thermal expansion (anharmonicity), *2*) be independent of force fields of unknown quality, *3*) produce quantities, which may be compared to experimental information from other than diffraction experiments, and *4*) be reasonably simple to use. A scheme fulfilling some of these conditions has recently been reported [11], implemented in a computer program [12][13] and tested on benzene, urea [14], and hexamethylenetetramine [15]. Qualitative aspects of the scheme are summarized here; some algebraic details are given in the *Experimental* (see *Models of Motion*). The model of motion assumes molecules moving in a harmonic average crystal field. There are three contributions to the ADPs: *1*) Those from low-frequency normal modes composed of molecular librations and translations *as well as* soft intramolecular deformations, such as torsions or out-of-plane motions. In the harmonic approximation, the contributions of these modes to the ADPs are constant at

low temperature and become proportional to temperature at higher temperatures (zero-point-motion and classical regimes). In practice, the frequencies decrease or increase smoothly, as the unit-cell expands or contracts with temperature (quasi-harmonic or *Grüneisen* model) [16]. *2*) Contributions from high-frequency normal modes which do not change significantly in the temperature range for which experimental information is available. *3*) Contributions unrelated to motion, *e.g.*, due to disorder and systematic error.

This description of ADPs is closely related to *Einstein*'s model, in which it is assumed that the positional displacements of atoms in a crystal are independent of each other and governed by an effective, local harmonic potential [17]. Here, *Einsteins*'s idea is applied to molecular coordinates. It turns out to be a useful approximation, not only for librations and deformations that tend to show relatively little intermolecular coupling (low dispersion in the *Brillouin* zone), but also for the much more strongly coupled molecular translations (acoustic phonons) [14][15].

Some aspects of this model are illustrated schematically in *Fig. 1*. The mean-square amplitude of a simple harmonic oscillator as a function of temperature is shown in *Fig. 1,a*. Its high-temperature branch extrapolates to zero at zero temperature, and its slope s at high temperature is related to the zero-point amplitude δ_0[1]). The temperature at which the zero-point amplitude equals the classical amplitude corresponds to half the *Einstein* temperature. If the linear high-temperature branch extrapolates to a positive value, a constant contribution ε is indicated (*Fig. 1,b*). If the increase in the mean-square amplitude at high temperature deviates from linearity, the oscillator frequency depends on temperature (*Fig. 1,c*). The general description of the mean-square amplitudes $\langle u^2 \rangle$ is given by

$$\langle u^2 \rangle = \hbar/(2\omega\mu) \coth(\hbar\omega/2k_BT) + \varepsilon \quad (1)$$

The oscillator frequency ω may depend on temperature T according to $\omega = \omega_0(1 - cT)$ with c describing the influence of thermal expansion. The reduced mass of the oscillator is given by μ; $\hbar$ and k_B are the usual constants. At least three measurements are necessary to determine the three quantities ω, c, and ε characterizing the temperature dependence of $\langle u^2 \rangle$ in the general case, two are sufficient if thermal expansion is negligible ($c = 0$).

The second limitation encountered in analyzing ADPs from a single or from multiple temperatures is the lack of information on the phases of the atomic displacements. This is especially constraining for nonrigid molecules where the amplitudes of molecular-deformation are comparable in magnitude to those of libration and translation. It has been shown elsewhere that, for the molecular crystal-field model discussed here, the combination of measurements in the zero-point and classical regimes do provide information, albeit in an indirect way, on these phases [11][18].

On this background, the ADPs of anthracene and naphthalene reported by *Brock* and co-workers [8–10] were interrogated with respect to the following points: *1*) Is an

---

[1]) The relationship is $s/\delta_0^2 = 4\,\mu\,k_B/\hbar$, μ is the effective mass of the oscillator, k_B is the *Boltzmann* constant and $\hbar$ is *Planck*'s constant.

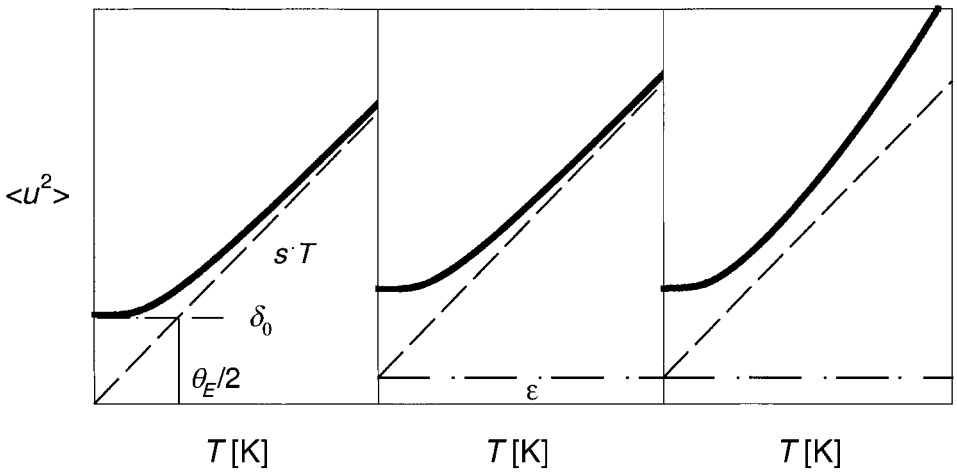

Fig. 1. *Mean-square amplitudes of vibration as a function of temperature for* a*) harmonic oscillator* (solid line) *with zero-point motion amplitudes* δ_o (short dashed line) *and amplitude of classical motion* s·T *with slope* s (dashed line; δ_o and $s \cdot T$ intersect at half the *Einstein* temperature $\theta_E/2$); b*) the sum of a harmonic oscillator and a temperature-independent term* ε (dash-dotted line); c*) the sum of an anharmonic oscillator and a temperature-independent term*

Einstein model capable of explaining the ADPs reported for all temperatures? *2*) Is a rigid-body model sufficient? *3*) What is the effect of thermal expansion? *4*) What are the amplitudes due to high-frequency intramolecular vibrations, and how do they compare with those from vibrational force fields? *5*) Are there systematic discrepancies between observed and calculated ADPs indicating shortcomings of the diffraction experiments or of the interpretation of the experimental data, *e.g.*, how are the ADPs affected by the choice of atomic scattering factors? At the end of the analysis, we hope to have shown that a consistent interpretation of all data with a single model reveals information that is impossible or very difficult to find from the ADPs at individual temperatures.

Experimental. – *Data*. X-Ray diffraction data for anthracene have been measured at 94, 140, 181, 220, 259, and 295 K to $\sin\theta/\lambda < 0.65$ A^{-1} [8]. At each temp., a model based on spherical atomic scattering factors, anisotropic ADPs for C, isotropic ADPs for H, and a weighting scheme based on counting statistics $w = w_{exp}$ was reported. There are 282 independent ADP data. The standard uncertainties of the diagonal parameters are between 0.0008 and 0.0014 A^2.

X-Ray diffraction data for naphthalene have been measured at 92, 109, 143, 184, and 239 K to $\sin\theta/\lambda <$ 0.65 A^{-1} [9]. At each temp., a model based on spherical atomic-scattering factors, anisotropic ADPs for C, isotropic ADPs for H, and an exponential weighting scheme $w = w_{exp} \cdot \exp[a(\sin\theta/\lambda)^2]$ was reported. There are 170 independent ADP data. The standard uncertainties of the diagonal parameters are between 0.0003 and 0.0007 A^2.

Both data sets have been rerefined with multipole parameters transferred from perylene [10]. The weighting scheme was $w^{-1} = \sigma^2(F^2) + (pF^2)^2$ with $p = 0.03$ and 0.02 for naphthalene and anthracene, resp. The ADPs were expressed as $\mathbf{U} = \mathbf{A}\ \mathbf{L}\ \mathbf{A}^T + \mathbf{T} + \mathbf{U}_{int}$, where **L** and **T** are the molecular libration and translation tensors, resp. [5], **A** is the matrix $[0, z - y, -z\ 0\ x, y - x\ 0]$ of atomic coordinates x, y, z, and $\mathbf{U}_{int}$ are the mean-square displacement amplitudes due to intramolecular vibrations. The components of **L** and **T** were refined, those of $\mathbf{U}_{int}$ were taken from a force-field calculation. The standard uncertainties of the diagonal elements of **T**

are between 0.0018 and 0.0029 A^2 for naphthalene, and 0.0018 and 0.0048 A^2 for anthracene, those of **L** are between 0.11 and 0.54 deg^2 for naphthalene, and between 0.1 and 0.9 deg^2 for anthracene. Because the analysis program used in this work requires ADPs as input, these were reconstructed from the reported **L** and **T** tensor elements in the crystal-axes system and from $\mathbf{U}_{int}$. The **U**s of the H-atoms were converted to isotropic values to take into account that these quantities are poorly determined from X-ray diffraction data. Standard uncertainties were chosen to be the same as for spherical atom ADPs. Although absolute uncertainties are too large by about a factor of three, their relative values should be approximately right.

(D_{10})Anthracene has been studied by neutron diffraction at 16 and 295 K [19][20]. The standard uncertainties of the 144 independent, anisotropic ADPs are 0.001 and 0.0006 A^2 for C, and 0.001 and 0.0011 A^2 for D.

(D_8)Naphthalene has been studied by neutron diffraction at 12 and 295 K [21] [22]. The 331 reflection intensities measured at r.t. were originally interpreted in terms of an **L** and a **T** tensor, and without taking into account the substantial zero-point amplitudes of D. For the purpose of this work, the data were rerefined anisotropically. Bond distances related by molecular *mm*-symmetry were restrained to be equal with $\sigma =$ 0.005 Å, 1,3-distances from D(2) and D(4) (bond angles) with $\sigma = 0.01$ Å and planarity with $\sigma = 0.01$ Å. After including an extinction coefficient (0.026(3)), refinement of 83 parameters converged at $R = 0.032$ (unit weights). ADPs and coordinates are listed at the end of the paper in *Table 8*. The standard uncertainties of the 108 independent ADPs are between 0.001 and 0.003 A^2 for C, and between 0.002 and 0.004 A^2 for D.

Models of motion take into account local low-frequency vibrations (molecular translation, libration, and some deformations), high-frequency vibrations (molecular-deformations), mixing of the soft molecular-deformation coordinates with the low-frequency translation and libration coordinates, and decrease of effective frequencies with increasing temp. due to thermal expansion of the crystal [11]. The explicit expression is

$$\Sigma^x(T) = \mathbf{A}\,\mathbf{g}\,\mathbf{V}\,\delta(T)\,\mathbf{V}^T\,\mathbf{g}^T\,\mathbf{A}^T + \boldsymbol{\varepsilon} \tag{2}$$

where $\delta(T)$ is a diagonal matrix with elements $\delta_i = \hbar/(2\omega_i)\coth(\hbar\omega_i/2k_BT)$, which represent the temp.-dependent mean-square amplitudes of local normal modes. **V** is an eigenvector matrix that transforms normal modes into mass-weighted molecular librations, translations, and deformations. The matrix **g** performs the mass correction, and **A** transforms the molecular into atomic displacements Σ^x. The matrix $\boldsymbol{\varepsilon}$ is a temperature-independent correction term. The diagonal 3×3 blocks of Σ^x correspond to the ADPs derived from the diffraction data, the off-diagonal 3×3 blocks correspond to interatomic correlation amplitudes and cannot be obtained from elastic diffraction experiments. Some features of this model are specially mentioned here, because they may not be apparent from the formula above: *1*) ADPs at all temperatures are expressed in terms of a single set of frequencies ω_i, eigenvectors **V** and $\boldsymbol{\varepsilon}$s. *2*) The eigenvector matrix **V** may be rectangular if the number of molecular coordinates needed to represent the normal coordinates is larger than the number of the latter. *3*) Thermal expansion of the crystal is taken into account through a *Grüneisen* correction γ_i to the effective frequencies: $\omega_i = \omega_{0i}\,(1 - \gamma_i\,\Delta V(T)/V_{min})$ where $\Delta V(T) = V(T) - V_{min}$, $V(T)$ is a polynomial expansion of the unit-cell volume V in T, and V_{min} is the unit-cell volume at the lowest available temperature [15]. *4*) The temp. independent term $\boldsymbol{\varepsilon}$ is taken to be the same for chemically equivalent or nearly equivalent atoms. It is anisotropic for C and H, isotropic for H. A common $\boldsymbol{\varepsilon}_{all}$, which is the same for all atoms, is sometimes needed to account for factors independent of atomic motion. *5*) The frequencies ω_i, the elements of **V** and the 3×3 diagonal blocks of $\boldsymbol{\varepsilon}$ are determined from multitemperature ADPs by a least-squares procedure with program NKA [12][13].

Coordinate Systems. All sets of ADPs were analyzed in molecular inertial coordinate systems calculated at each temp. separately. The *x*-axes coincide with the long dimension of the molecules, the *y*-axes are orthogonal to the *x*-axes in the molecular plane, and the *z*-axes are orthogonal to *x* and *y*. C(1) is in the $-x/+y$ quadrant (*Fig. 2*). The $\boldsymbol{\varepsilon}$-tensors are expressed in local atomic-coordinate systems with their *x*-axes along C–H/D bonds (C_2C–H/D) or exocyclic C–C–C bisectors (C_2C–C), their *y*-axes in the molecular plane and their *z*-axes perpendicular to it.

Normal-Mode Calculations by Density-Functional Theory (DFT). Molecular geometries were optimized with a B3LYP functional using a 6-31G** basis set. Normal mode frequencies and eigenvectors were calculated for H- and D-isotopomers from analytical second derivatives. Both calculations were performed with the program package GAUSSIAN98. Intramolecular atomic mean-square amplitudes were calculated with an expression analogous to *Eqn. 2*. Calculated frequencies agree within expected limits with scaled results from HF/6-31G* calculations and unscaled results from BLYP/6-31G** calculations on anthracene [23][24]. Similar agreement is found at several levels of theory for naphthalene [25].

Results. – *Models of Motion*. Four different models have been fitted to the ADPs. The first one corresponds to rigid-body motion with librational coordinates l_x, l_y, and l_z, translational coordinates t_x,t_y, and t_z, a common *Grüneisen* constant for all six normal modes and separate εs for C and H/D (model RB, 20/25 parameters). In the second model, a constant contribution ε_{all} is added to the ADPs of all atoms in addition to the individual atomic εs (model RB (ε_{all}), 24/29 parameters). In the third model, an out-of-plane bending coordinate b_{1u} is allowed to mix into the translational degrees of freedom. It deforms the molecule into an arc spanning the *x*-axis. Relative atomic displacements were taken from the corresponding mode in the gas phase as calculated by DFT (model RB(b_{1u}, ε_{all}), 27/32 parameters). The fourth model includes two extra motions, the out-of-plane bending modes b_{1u} and a_u corresponding to the arc-deformation mentioned above and a twist-deformation about the long axes of the molecules (model RB, b_{1u}, a_u (ε_{all}), 26/31 parameters). They are the two lowest-frequency molecular-deformations.

The effective frequencies, *Grüneisen* constants, *R* values, and goodness-of-fit (GOF) of the four models are summarized in *Table 1* for anthracene and naphthalene.

Table 1. *Frequencies of Local Normal Modes for Different Models of Motion from X-Ray-Diffraction Data* (in brackets: predominant character of eigenvectors or standard uncertainties), Grüneisen *Parameter* γ; R *Factors and Goodness-of-Fit (GOF)*

	$\nu(l_x)$ [cm^{-1}]	$\nu(l_y)$ [cm^{-1}]	$\nu(t_z)$ [cm^{-1}]	$\nu(l_z)$ [cm^{-1}]	$\nu(t_x)$ [cm^{-1}]	$\nu(t_y)$ [cm^{-1}]	γ	$wR2$[a] [%]	GOF[a]
	Anthracene								
RB[b]	108.0(20)	63.4(4)	45.0(3)	48.9(3)	36.5(2)	45.7(3)	3.3(1)	2.8	–
	116.5(54)	61.1(8)	42.8(6)	47.5(5)	34.0(4)	41.6(5)	2.6(2)	4.3	0.98
RB(ε_{all})	108.1(16)	63.5(3)	45.7(3)	48.4(2)	36.9(2)	44.5(3)	3.3(1)	2.2	–
	117.0(52)	61.1(8)	43.0(6)	47.1(5)	34.3(4)	41.3(5)	2.6(2)	4.1	0.93
RB(b_{1u}, ε_{all})	104.7(11)	47.0(2)	56.3(5)	50.4(3)	36.8(1)	44.6(2)	3.3(1)	1.6	–
	100.3(33)	44.2(6)	55.1(11)	48.3(6)	33.9(3)	40.7(5)	2.5(2)	3.7	0.85
RB, b_{1u}, a_u	114.6(30)	71.0(10)	48.5(3)	49.0(2)	37.4(1)	45.5(2)	3.5(1)	1.6	–
(ε_{all})	b_{1u}		97(4)	a_u		123(8)			
	99.9(38)	64.2(10)	47.3(7)	47.2(5)	34.2(4)	41.2(5)	2.6(2)	3.9	0.88
	b_{1u}		95(4)	a_u		(132)[c]			
	Naphthalene								
RB[b]	122.9(28)	77.5(7)	54.8(4)	55.2(4)	44.3(3)	52.2(4)	3.3(1)	2.9	–
	117.2(30)	79.3(9)	60.1(7)	56.0(5)	48.7(4)	58.3(6)	4.1(2)	3.8	1.29
RB(ε_{all})	125.6(11)	79.0(3)	55.7(2)	56.8(2)	46.3(3)	54.6(2)	3.7(1)	1.1	–
	119.8(24)	80.8(7)	61.8(5)	57.9(4)	50.7(4)	60.6(5)	4.5(1)	2.9	1.00
RB	98.5(27)	58.3(10)	76.9(31)	56.6(2)	46.1(1)	54.7(2)	3.6(1)	1.1	–
(b_{1u}, ε_{all})	119.3(19)	80.9(9)	62.3(7)	57.7(4)	50.6(3)	60.2(5)	4.5(1)	2.7	0.93
RB, b_{1u}, a_u	119.3(13)	79.8(3)	58.2(3)	57.0(2)	46.5(1)	55.2(2)	3.8(1)	1.1	
(ε_{all})	b_{1u}		(174)[d]	a_u		(191)[e]			–
	117(15)	82.3(30)	65.3(33)	58.1(5)	51.0(4)	61.4(6)	4.6(1)	2.8	0.96
	b_{1u}		166(67)	a_u		163(38)			

[a]) $wR2 = \{\Sigma[\Delta U^2/\sigma^2(U)]/\Sigma[U^2/\sigma^2(U)]\}^{1/2}$, $\mathrm{GOF} = \{\Sigma[\Delta U^2/\sigma^2(U)]/(n_{obs} - n_{par})\}^{1/2}$.

[b]) First line: ADP's from multipole refinement; second line: ADP's from spherical-atom refinement.

[c]) Restrained to 124 cm^{-1} with $\sigma = 10$ cm^{-1}.

[d]) Restrained to 177 cm^{-1} with $\sigma = 10$ cm^{-1}.

[e]) Restrained to 190 cm^{-1} with $\sigma = 10$ cm^{-1}.

Pairs of lines refer to ADPs from multipole and spherical-atom refinements, respectively (see *Experimental*). The 282 carbon ADPs of anthracene (150 for naphthalene) are explained by rigid-body motion to the extent of 95% or better (model RB, $wR2 < 5\%$), indicating that the simple *Einstein* model represents the temperature dependence of ADPs quite well and implying a significant economy of description. Only 20 parameters are needed to describe the ADPs of anthracene and naphthalene instead of the 72 and 60 components of **T** and **L** used previously.

One could be quite satisfied with this result and move on to the next problem, if it were not for the fact that a graphical representation of the differences $\Delta\mathbf{U}$ between observed and model ADPs show systematic features. This is illustrated for anthracene in *Fig. 2* (*left*): first, the $\Delta\mathbf{U}$'s for most atoms at 94 K are very similar. The differences at 140 and 181 K seem to continue this trend, although to a lesser extent. Second, the differences perpendicular to the molecular plane are systematically positive for C(1), C(4), and C(7), and negative for C(2), C(3), C(5), and C(6) at the four higher temperatures. They indicate motion not included in the minimal rigid-body model and are likely to be related to the low-frequency molecular-deformation modes found spectroscopically (b_{1u} 106 cm^{-1}, a_u 142 cm^{-1} [26][27]) and from DFT calculations (b_{1u} 94 cm^{-1}, a_u 124 cm^{-1}).

The first feature has been parametrized with the help of a temperature-independent contribution $\boldsymbol{\varepsilon}_{\text{all}}$, which is the same for all atoms (model RB($\boldsymbol{\varepsilon}_{\text{all}}$), with components $\varepsilon_{11} = -\varepsilon_{22} = 0.0009(1)$, $\varepsilon_{33} = 0$ (fixed), $\varepsilon_{12} = 0.0003(1)$, $\varepsilon_{13} = 0.0011(1)$, $\varepsilon_{23} = 0.0001(1)$). The four extra parameters improve the fit significantly without seriously affecting the rest of the model. The possible significance of $\boldsymbol{\varepsilon}_{\text{all}}$ is discussed below (see *Temperature-Independent Contributions to the ADPs*). The second feature was interpreted either in terms of an arc-shaped deformation coupled primarily to translation in the z-direction ($t_z + b_{1u}$), or two additional normal modes, an arc-shaped and a twist deformation (b_{1u}, a_u). In both cases, the extra parameters improve the fit significantly. *Fig. 2* (*right*) shows that, for the model RB, b_{1u}, a_u ($\boldsymbol{\varepsilon}_{\text{all}}$), the $\Delta\mathbf{U}$s are smaller and less systematic than for model RB. The last two models differ in the description of the motions out of the molecular plane and show differences in the corresponding frequencies $\nu(l_x)$, $\nu(l_y)$, and $\nu(t_z)$, whereas the in-plane part of the model does not change much ($\nu(l_z)$, $\nu(t_x)$, and $\nu(t_y)$).

The two models RB(b_{1u}, $\boldsymbol{\varepsilon}_{\text{all}}$) and RB, b_{1u}, a_u ($\boldsymbol{\varepsilon}_{\text{all}}$) explain the multipole data of anthracene about equally well; R factors and GOF are nearly the same. This lack of discrimination is probably related to the restricted temperature range covered by the data, 94 to 295 K. They do not include the zero-point-motion regime, which is crucial to the determination of the phases of atomic displacements. The frequencies of the intramolecular deformation modes of the model RB, b_{1u}, a_u ($\boldsymbol{\varepsilon}_{\text{all}}$) are poorly determined, although their magnitudes happen to be close to the spectroscopic and DFT values. Data at very much lower temperatures would probably help here too. The results from spherical atom ADPs are similar, except that the twist-deformation frequency refines to a very high value unless it is weakly restrained (*Table 1*).

The results for naphthalene are less conclusive than those for anthracene (*Table 1*). The general term $\boldsymbol{\varepsilon}_{\text{all}}$ is again significant ($\varepsilon_{11} = -\varepsilon_{22} = -0.0004(1)$, $\varepsilon_{33} = 0$ (fixed), $\varepsilon_{12} = -0.0009(1)$, $\varepsilon_{13} = -0.0018(1)$, $\varepsilon_{23} = -0.0005(1)$), but the two models RB(b_{1u}, $\boldsymbol{\varepsilon}_{\text{all}}$) and RB, b_{1u}, a_u ($\boldsymbol{\varepsilon}_{\text{all}}$) are no better than the simpler model RB($\boldsymbol{\varepsilon}_{\text{all}}$). With the multipole-

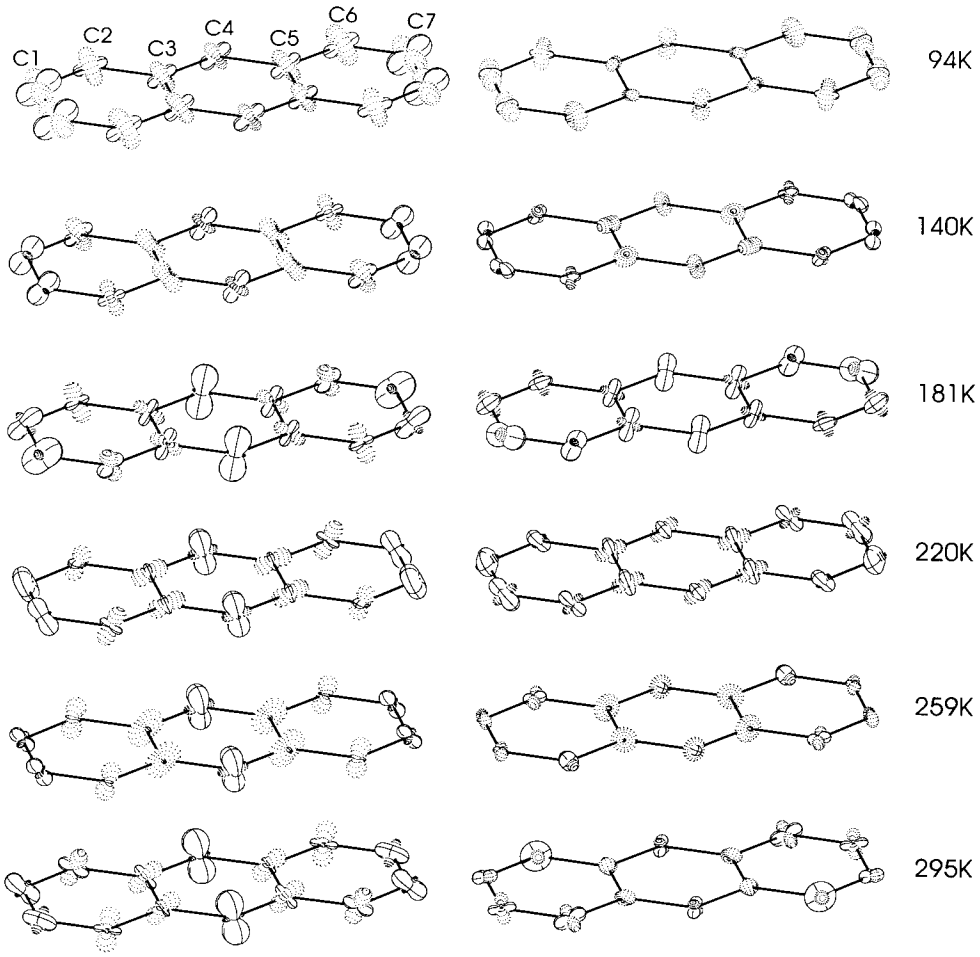

Fig. 2. *PEANUT plots of* $\mathbf{U}_{obs} - \mathbf{U}_{calc}$ *for a simple rigid-body model fitted to the ADPs of anthracene from multipole refinement* (left) *and for the model including* ε_{all}, *arc- and twist-deformations* b_{1u} *and* a_u (right). Atoms related through the crystallographic center of symmetry are not numbered but referred to by primed symbols. The molecular *x*-axis points along the long direction of the molecule towards C(1), the *y*-axis points towards C(4). The atomic numbering of the naphthalene molecule is analogous.

derived ADPs the two extra frequencies in model RB, b_{1u}, a_u ($\boldsymbol{\varepsilon}_{all}$) refine to unreasonably low and high values, respectively, and have, therefore, been fixed at their DFT values. With the spherical-atom-derived ADPs, the two frequencies happen to refine to reasonable values, but their standard uncertainties are enormous, a quarter to a third of the frequencies themselves. This lack of information in the naphthalene data is consistent with the facts that *1*) the naphthalene ADPs cover an even smaller temperature range than those of anthracene, 92 to only 239 K, and *2*) the two lowest intramolecular deformation frequencies of naphthalene are significantly higher than those of anthracene (b_{1u} 177 cm^{-1}, a_u 190 cm^{-1}, from DFT calculations). The lower limit

of temperature corresponds to about half the *Einstein* temperatures, the upper limit is just below the *Einstein* temperatures of these modes (b_{1u} 255 K, a_u 274 K, from DFT calculations). This range is insufficient to fix these frequencies.

The *Grüneisen* constants seem to depend on the way the diffraction data have been refined (*Table 1*): they are *ca*. 2.5 for the standard spherical-atom refinement of anthracene, but *ca*. 4.5 for the corresponding refinement of naphthalene, in which the weights of the reflection intensities were increased with increasing scattering angle by multiplication with the function $\exp[a(\sin\Theta/\lambda)^2]$. The *Grüneisen* constants derived from the multipole ADPs are very similar for both compounds, *ca*. 3.5. This value is of the right order of magnitude, but somewhat higher than found previously for hexamethylenetetramine (2.3) [15]. It seems likely that part of the increase is due to the hydrocarbon nature of anthracene and naphthalene, and part to the limited temperature and resolution ranges covered by the respective diffraction data.

Isotope Effects. For (D_{10})anthracene the models RB(b_{1u}, $\boldsymbol{\varepsilon}_{all}$) and RB, b_{1u}, a_u ($\boldsymbol{\varepsilon}_{all}$) can be discriminated with the help of the 144 ADPs of C and D determined by neutron diffraction at 16 and 295 K. In all four models described above, $\boldsymbol{\varepsilon}_{all}$ was found to be insignificant. The *Grüneisen* constant had to be fixed at the value found from the X-ray data, because the neutron data pertain to two temperatures only. The fit for the model RB, b_{1u}, a_u with independent arc- and twist-deformation modes, is best (*Table 2*). Corresponding results for (D_8)naphthalene are of lesser quality, as may be seen from the generally higher *R* factors. Although the model RB(b_{1u}, $\boldsymbol{\varepsilon}_{all}$) seems slightly favored over model RB, b_{1u}, a_u ($\boldsymbol{\varepsilon}_{all}$) from the point of view of overall agreement, the isotopic ratios discussed in the next paragraph lead to the opposite conclusion.

The models derived from H and D data may be compared *via* the ratios of corresponding frequencies. Strictly speaking, the product of the ratios ν^H/ν^D of the *gerade* and *ungerade* frequencies, respectively, should be compared with the corresponding products of reduced mass ratios. In the present case, the motions corresponding to the quasi-normal modes correspond very closely to l_x, l_y, l_z, t_x, t_y, t_z, b_{1u}, and a_u respectively. It is, therefore, a good approximation to compare the ratio of frequencies with ratios of corresponding inertial moments $(I^D/I^H)^{1/2}$, molecular weights $(M^D/M^H)^{3/2}$ and ratios of frequencies ν^H/ν^D from DFT calculations (*Table 2*).

The isotopic ratios deduced from diffraction data differ systematically from expected values. They tend to be too large for librations, and too small for translations. In the case of anthracene, the isotopic ratios do not allow discrimination between the two models. In the case of naphthalene, the model including an arc-shaped deformation, (RB(b_{1u}, $\boldsymbol{\varepsilon}_{all}$)) shows larger deviations from expected values than the model with two additional modes (RB, b_{1u}, a_u, ($\boldsymbol{\varepsilon}_{all}$)), expecially for the libration about the *y*-axis l_y which shows a ratio of clearly < 1, and for the translation along *z*, t_z, which shows a ratio $>> 1$. Overall, the analysis of the deuterated molecules indicate a slight preference for the model with intramolecular b_{1u} and a_u deformations for anthracene and probably also for naphthalene.

Temperature-Independent Contributions to the ADPs. Two such contributions have been refined from the ADP data. The first, $\boldsymbol{\varepsilon}_{all}$, affects all atoms equally and is intended to account for contributions to the ADPs arising from systematic errors in the diffraction data. Its use and effect on the least-squares refinements have been illustrated above for the various models and data sets. Its interpretation in terms of

Table 2. *Frequencies of Local Normal Modes for Different Models of Motions from Neutron-Diffraction Data and Isotopic Ratios* (in brackets: predominant character of eigenvectors or standard uncertainties); Grüneisen *Parameter* γ; R *Factors and Goodness-of-Fit* (*GOF*)

	$\nu(l_x)$ [cm^{-1}] ν^H/ν^D	$\nu(l_y)$ [cm^{-1}] ν^H/ν^D	$\nu(t_z)$ [cm^{-1}] ν^H/ν^D	$\nu(l_z)$ [cm^{-1}] ν^H/ν^D	$\nu(t_x)$ [cm^{-1}] ν^H/ν^D	$\nu(t_y)$ [cm^{-1}] ν^H/ν^D	γ (fixed	R[a]) [%]	GOF[a])
	(D_{10})Anthracene								
RB	83.9(16)	54.7(5)	49.0(7)	45.4(3)	36.9(2)	46.4(5)	3.3	4.2	1.42
	1.29(3)	1.16(1)	0.93(2)	1.07(1)	1.00(1)	0.98(1)			
RB(b_{1u})	81.5(14)	44.8(4)	61.2(19)	46.7(5)	36.9(2)	46.7(5)	3.3	3.8	1.31
	1.28(2)	1.05(1)	0.92(4)	1.08(1)	1.00(1)	0.96(1)			
RB, b_{1u}, a_u	89.1(21)	61.8(8)	51.5(8)	45.9(2)	37.3(1)	47.1(4)	3.5	3.4	1.12
	1.29(4)	1.15(2)	0.94(2)	1.07(1)	1.00(1)	0.97(1)			
	b_{1u}	101(4)		a_u	124(7)				
		0.97(5)			0.99(9)				
Expected	1.09	1.10	1.06	1.11	1.06	1.06			
ratios[b])	b_{1u}	1.06		a_u	1.10				
	(D_8)Naphthalene								
RB	93.7(60)	66.5(26)	56.2(21)	50.0(12)	40.7(7)	53.4(19)	3.7	13.1	2.46
	1.31(7)	1.17(4)	0.98(4)	1.10(3)	1.09(2)	0.98(4)			
RB(ε_{all})	93.4(32)	66.7(14)	57.5(11)	50.6(7)	39.8(4)	54.3(12)	3.7	7.0	1.32
	1.35(4)	1.18(2)	0.97(2)	1.12(1)	1.16(1)	1.01(2)			
RB	94.2(46)	71.9(69)	52.9(25)	49.2(7)	39.8(3)	58.6(21)	3.7	6.5	1.24
(b_{1u}, ε_{all})	1.05(6)	0.82(12)	1.45(8)	1.15(2)	1.16(1)	0.93(4)			
RB, b_{1u}, a_u	95.7(37)	70.1(17)	54.9(12)	50.7(7)	39.9(3)	57.8(12)	3.7	6.9	1.29
(ε_{all})	1.25(4)	1.14(3)	1.06(2)	1.12(1)	1.17(1)	0.96(2)			
	b_{1u}	192(42)		a_u	(172) [c])				
Expected	1.09	1.06	1.03	1.07	1.03	1.03			
ratios[b])	b_{1u}	1.08		a_u	1.10				

[a]) $wR2 = \{\Sigma[\Delta U^2/\sigma^2(U)]/\Sigma[U^2/\sigma^2(U)]\}^{1/2}$, $GOF = \{\Sigma[\Delta U^2/\sigma^2(U)]/(n_{obs} - n_{par})\}^{1/2}$.
[b]) $(I^D/I^H)^{1/2}$ for librations, $(M^D/M^H)^{1/2}$ for translations, ν^H/ν^D for intramolecular modes.
[c]) Restrained to 171 cm^{-1} with $\sigma = 10$ cm^{-1}.

systematic error, rather than motion, is discussed below. The second, ε(C, H, or D), is specific for each group of chemically similar atoms and is intended to represent the mean-square amplitudes of intramolecular motion arising from the higher-frequency deformation modes, those that are not significantly excited in the temperature range of the experiments.

The intramolecular mean-square amplitudes derived from X-ray diffraction data of anthracene are compared with those calculated by DFT in *Table 3*. The amplitudes in the molecular plane, ε_{11} and ε_{22}, obtained from the spherical-atom refinements are systematically and consistently larger than those from multipole refinements and DFT calculations, by *ca.* 0.003 Å^2 on average. Conversely the amplitudes perpendicular to the molecular plane, ε_{33}, tend to be systematically smaller. The differences simulate the well-known fact that spherical-atom refinements parametrize the aspherical nature of the valence-electron density, due to bonding effects, in terms of additions to the ADPs, whereas multipole refinements account for such asphericity by explicit multipolar functions. Here, a transfer of charge from the region above the atoms into the regions of the chemical bonds to their neighbors is observed.

Table 3. *Anthracene: Temperature-Independent Mean-Square Amplitudes from X-Ray-Diffraction Data and Intramolecular Mean-Square Amplitudes from DFT Calculations*[a])

	ε_{11} ($\cdot 10^4$ Å^2)	ε_{22} ($\cdot 10^4$ Å^2)	ε_{33} ($\cdot 10^4$ Å^2)
RB(b_{1u}, $\boldsymbol{\varepsilon}_{\text{all}}$)			
all C-atoms[b])	9(1)	9(1)	20(1)
C(1), C(2), C(4), C(6), C(7)[c])	32(2)	71(3)	7(4)
C(3), C(5)[c])	49(3)	48(3)	4(4)
RB, b_{1u}, a_u ($\boldsymbol{\varepsilon}_{\text{all}}$)			
all C-atoms[b])	13(1)	14(1)	12(1)
C(1), C(2), C(4), C(6), C(7)[c])	34(3)	74(3)	−2(4)
C(3), C(5)[c])	51(3)	51(3)	0(4)
DFT Calculations			
C(1), C(7)	16, 19[d])	14, 19[d])	17 (56), 24 (130)[e])
C(2), C(6)	15, 16	16, 20	19 (40), 26 (79)
C(3), C(5)	16, 21	12, 13	23 (39), 31 (75)
C(4)	17, 22	13, 14	23 (48), 34 (103)

[a]) ε_{11} along C–H (or C(3)–C(5′)); ε_{22} in plane, ε_{33} out of plane, see *Fig. 2*.
[b]) ADPs from multipole refinement.
[c]) ADPs from spherical-atom refinement.
[d]) First number: 94 K, second number: 295 K.
[e]) Numbers without brackets: contribution from all but the lowest two frequencies at 94 and 295 K; numbers in brackets: contributions from all frequencies at 94 and 295 K.

The ε values from multipole refinement tend to agree better with the ε values from DFT calculations than those from spherical atom refinements. The in-plane components are close to the values calculated at the lowest experimental temperature (94 K). The out-of-plane components are comparable to the DFT values at 94 K provided the contributions from lowest two intermolecular frequencies are not included. The effect of these frequencies is accounted for implicitly (model RB(b_{1u}, $\boldsymbol{\varepsilon}_{\text{all}}$)) or explicitly (model RB, b_{1u}, a_u ($\boldsymbol{\varepsilon}_{\text{all}}$)) in the temperature-dependent part of the model of motion (see above). Note that the contribution of these frequencies is substantial, and their increase with temperature much more pronounced than those of the remaining 19 out-of-plane vibrations. The comparison for (D_{10})anthracene gives similar results (*Table 4*). The ε values from the neutron-diffraction data are close to those calculated at the lowest experimental temperature (16 K) for both C- and D-atoms. The calculated temperature dependence of the contribution from the 19 higher-frequency out-of-plane vibrations is distinctly more pronounced for the D- than for the C-atoms, and also much larger than the standard uncertainty of the ADPs (0.001 Å^2). It seems likely that this increase, which cannot be absorbed into a temperature-independent $\boldsymbol{\varepsilon}$, has been included in the libration modes $\nu(l_x)$ and $\nu(l_y)$ whose frequencies may, therefore, well be too low, in agreement with the unusually high isotopic ratios reported in *Table 2*.

The results for naphthalene are similar to those for anthracene (*Tables 5* and *6*). The in-plane ε values from spherical-atom refinements are too large and about the same as for anthracene. Corresponding $\boldsymbol{\varepsilon}$'s from multipolar refinement tend to be somewhat larger than the calculated ones. The ε values from neutron diffraction agree with those calculated for (D_8)naphthalene. The out-of-plane $\boldsymbol{\varepsilon}$'s are all quite similar.

Table 4. *(D_{10})Anthracene: Temperature-Independent Mean-Square Amplitudes from Neutron-Diffraction Data and Intramolecular Mean-Square Amplitudes from DFT Calculations*[a])

	ε_{11} ($\cdot 10^4$ Å^2)	ε_{22} ($\cdot 10^4$ Å^2)	ε_{33} ($\cdot 10^4$ Å^2)
RB(b_{1u})			
all C-atoms	14(4)	16(3)	23(4)
all D-atoms	56(4)	116(4)	187(5)
RB, b_{1u}, a_u			
all C-atoms	14(3)	16(3)	17(3)
all D-atoms	56(3)	116(3)	145(5)
DFT Calculations			
C(1), C(7)	16, 20[b])	14, 19[b])	17 (39), 24(123)[c])
C(2), C(6)	15, 16	16, 20	20 (34), 27 (81)
C(3), C(5)	16, 21	13, 14	24 (33), 33 (77)
C(4)	18, 23	13, 14	24 (40), 36 (112)
D(1), D(7)	49, 52	106, 124	142 (211), 190 (503)
D(2), D(6)	47, 48	112, 135	143 (189), 183 (358)
D(4)	50, 55	106, 115	164 (178), 220 (289)

[a]) ε_{11} along C–D (or C(3)–C(5′)), ε_{22} in plane, ε_{33} out of plane, see *Fig. 2*.
[b]) First number: 16 K; second number: 295 K.
[c]) Numbers without brackets: contribution from all but the lowest two frequencies at 16 and 295 K; numbers in brackets: contributions from all frequencies at 16 and 295 K.

Table 5. *Naphthalene: Temperature-Independent Mean-Square Amplitudes from X-Ray-Diffraction Data and Intramolecular Mean-Square Amplitudes from DFT Calculations*[a])

	ε_{11} ($\cdot 10^4$ Å^2)	ε_{22} ($\cdot 10^4$ Å^2)	ε_{33} ($\cdot 10^4$ Å^2)
RB(b_{1u}, $\boldsymbol{\varepsilon}_{\text{all}}$)			
all C-atoms[b])	22(1)	22(1)	20(1)
all C-atoms[c])	46(1)	56(1)	27(1)
RB, b_{1u}, a_u, ($\boldsymbol{\varepsilon}_{\text{all}}$)			
all C-atoms[b])	24(1)	24(1)	13(1)
all C-atoms[c])	47(1)	58(2)	17(2)
DFT Calculations			
C(1), C(5)	15, 15[d])	11, 12[d])	12(28), 12(42)[d])[e])
C(2), C(4)	14, 15	13, 14	14(26), 15(37)
C(3)	15, 16	11, 12	17(31), 18(44)

[a]) ε_{11} along C–H (or C(3)–C(3′)), ε_{22} in plane, ε_{33} out of plane, see *Fig. 2*.
[b]) ADPs from multipole refinement.
[d]) ADPs from spherical-atom refinement.
[d]) First number: 92 K, second number: 239 K.
[e]) Numbers without brackets: contribution from all but the lowest two frequencies at 92 and 239 K; numbers in brackets: contributions from all frequencies at 92 and 239 K.

The temperature dependence of the calculated ε_{33} values of the D-atoms is somewhat less pronounced, as expected from the higher vibration frequencies of the lowest two out-of-plane vibrations (163 and 171 cm^{-1} for (D_8)naphthalene *vs.* 88 and 113 cm^{-1} for (D_8)anthracene), and well within the standard uncertainties of the neutron diffraction data at 295 K, which are of limited accuracy (see *Experimental* and *Table 8*). This and

Table 6. *(D_8)Naphthalene: Temperature-Independent Mean-Square Amplitudes from Neutron-Diffraction Data and Intramolecular Mean-Square Amplitudes from DFT Calculations*[a])

	ε_{11} ($\cdot 10^4$ Å^2)	ε_{22} ($\cdot 10^4$ Å^2)	ε_{33} ($\cdot 10^4$ Å^2)
RB(b_{1u}, $\boldsymbol{\varepsilon}_{all}$)			
all C-atoms	16(2)	18(2)	30(2)
all C-atoms	51(3)	89(3)	157(4)
RB, b_{1u}, a_u ($\boldsymbol{\varepsilon}_{all}$)			
all C-atoms	16(2)	18(2)	21(2)
all D-atoms	51(3)	89(3)	122(5)
DFT Calculations			
C(1), C(5)	14, 16[b])	11, 13[b])	13(25), 16(48)[c])
C(2), C(4)	14, 15	13, 14	15(26), 18(46)
C(3)	14, 17	12, 12	17(29), 20(52)
D(1), D(5)	47, 49	99, 107	118(178), 139(298)
D(2), D(4)	47, 48	105, 116	135(165), 165(244)

[a]) ε_{11} along C–D (or C(3)–C(3′)), ε_{22} in plane, ε_{33} out of plane, see *Fig. 2*.
[b]) First number: 12 K, second number: 295 K.
[c]) Numbers without brackets: contribution from all but the lowest two frequencies at 12 and 295 K; numbers in brackets: contributions from all frequencies at 12 and 295 K.

the limited temperature range for which X-ray data have been measured (92 to 239 K) would seem to preclude a more detailed interpretation of the results derived from the diffraction data on the two isotopomers of naphthalene.

To avoid singularities in the least-squares determination of $\boldsymbol{\varepsilon}_{all}$ for a planar molecule, it is necessary to constrain the sum of the two diagonal elements referring to the molecular plane and, independently, the element referring to the direction perpendicular to the molecular plane. The numbers in *Table 7* (*top*) lacking a standard uncertainty have been constrained accordingly. For $C_{14}D_{10}$ and $C_{10}D_8$, the diagonal elements of $\boldsymbol{\varepsilon}_{all}$ have been fixed such that the values of $\boldsymbol{\varepsilon}$(C) are reasonable. It has been suggested above that the role of $\boldsymbol{\varepsilon}_{all}$ in modeling the ADPs is to account for factors in the diffraction data that are poorly accounted for in the structure refinement (extinction, absorption, limited resolution). It is difficult to provide conclusive evidence for such an interpretation, but some indication in this direction follows if the $\boldsymbol{\varepsilon}_{all}$ are transformed from the molecular inertial coordinate system to the monoclinic crystal coordinate systems of anthracene and naphthalene, respectively. *Table 7* (bottom) shows that the off-diagonal elements $\varepsilon_{12\,and}$ ε_{23} tend to be small or insignificant compared to ε_{13} and the diagonal elements, *i.e.*, the tensor $\boldsymbol{\varepsilon}_{all}$ shows nearly monoclinic symmetry ($\varepsilon_{12} = \varepsilon_{23} = 0$). This is in agreement with the practice of averaging the measured intensities of different, but symmetry-equivalent reflections. Any remaining systematic errors in the averaged intensities necessarily show the symmetry used in averaging. The physical effects responsible for $\boldsymbol{\varepsilon}_{all}$ have not been investigated for the data discussed in this work, but see [28].

Discussion, Conclusions, and Outlook. – *Discussion*. The results of this study are compared with those of *Brock et al*. [10] in *Fig. 3*, which displays the diagonal elements of the molecular translation and libration tensors **T** and **L**. The individual points are from rigid-body analyses at single temperatures after correction for internal motion,

Table 7. *Temperature-Independent Contribution* $\boldsymbol{\varepsilon}_{all}$ *in Inertial* (top) *and Crystal Coordinate Systems* (bottom)

	ε_{11}	ε_{22}	ε_{33}	ε_{12}	ε_{13}	ε_{23}
$C_{14}H_{10}$ [a])	8(1)	−8	0	3(1)	11(1)	0(1)
[b])	8(1)	−8	0	6(1)	9(1)	0(1)
$C_{14}D_{10}$	15	15	0	0	0	0
$C_{10}H_8$ [a])	−4(1)	4	0	−9(1)	−18(1)	−5(1)
[b])	−6(1)	6	0	−10(1)	−15(1)	−1(1)
$C_{10}D_8$	26(1)	54	20	−6(2)	−24(1)	−15(2)
$C_{14}H_{10}$ [a])[c])	−3	−7	−4	−2	−11	−1
[b])[c])	−3	−6	−5	−2	−10	−4
$C_{14}D_{10}$ [d])	3	12	12	6	3	3
$C_{10}H_8$ [a])[e])	1	6	13	−6	−16	−1
[b])[e])	4	4	12	−2	16	3
$C_{10}D_8$ [f])	19	60	44	−1	32	1

[a]) Multipole data, model RB, b_{lu}, a_u ($\boldsymbol{\varepsilon}_{all}$).
[b]) Spherical-atom data, model RB, b_{lu}, a_u ($\boldsymbol{\varepsilon}_{all}$).
[c]) Transformation matrix from 140 K data.
[d]) Transformation matrix from 16 K data.
[e]) Transformation matrix from 143 K data.
[f]) Transformation matrix from 12 K data.

the continuous curves are from the global *Einstein* model. The separately evaluated out-of-plane components L_{11} and L_{22} are bigger, the T_{33} ones are smaller than those from the *Einstein* model. At 140, 259, and 295 K, relatively large positive differences in L_{11} and L_{22} are compensated by corresponding negative differences in T_{33}. This shows that the *Einstein* model subdivides the atomic out-of-plane amplitudes differently from the rigid-body analyses. We prefer the results from the *Einstein* model because, unlike those from rigid-body analysis, they are subject to the same physical boundary conditions at all temperatures. In addition, they are less susceptible to statistical outliers than are those from rigid-body analyses at individual temperatures, because, with the *Einstein* model, all ADPs are analyzed in a single least-squares calculation. The in-plane components L_{33}, T_{11}, and T_{22} compare well at all temperatures. In view of the minor temperature dependence of the intramolecular in-plane amplitudes ε_{11} and ε_{22} (*Table 3*), it is concluded that L_{33}, T_{11}, and T_{22} are close to the 'true' in-plane translation and libration amplitudes.

The quality of ADPs is often judged with the help of the so-called *Hirshfeld* test [29]: ADPs are deemed physically meaningful if the mean-square amplitudes along the internuclear vector of two more or less rigidly connected, usually bonded atoms are the same. The present analysis shows that this test can only be meaningful for ADPs from multipole refinements but not for ADPs from spherical atom refinements (*Tables 3* and *5*). In the former case, ADPs represent mostly vibrational motion, whereas in the latter they reflect motion *and* asphericity of bonding density. The latter may well be different for two bonded atoms with different chemical environments, thus invalidating the test.

Summary and Conclusions. The ADPs of anthracene and naphthalene derived from X-ray or neutron-diffraction data have been analyzed with an *Einstein* model including *1*) local normal modes such as librations, translations, and low-fequency out-of-plane

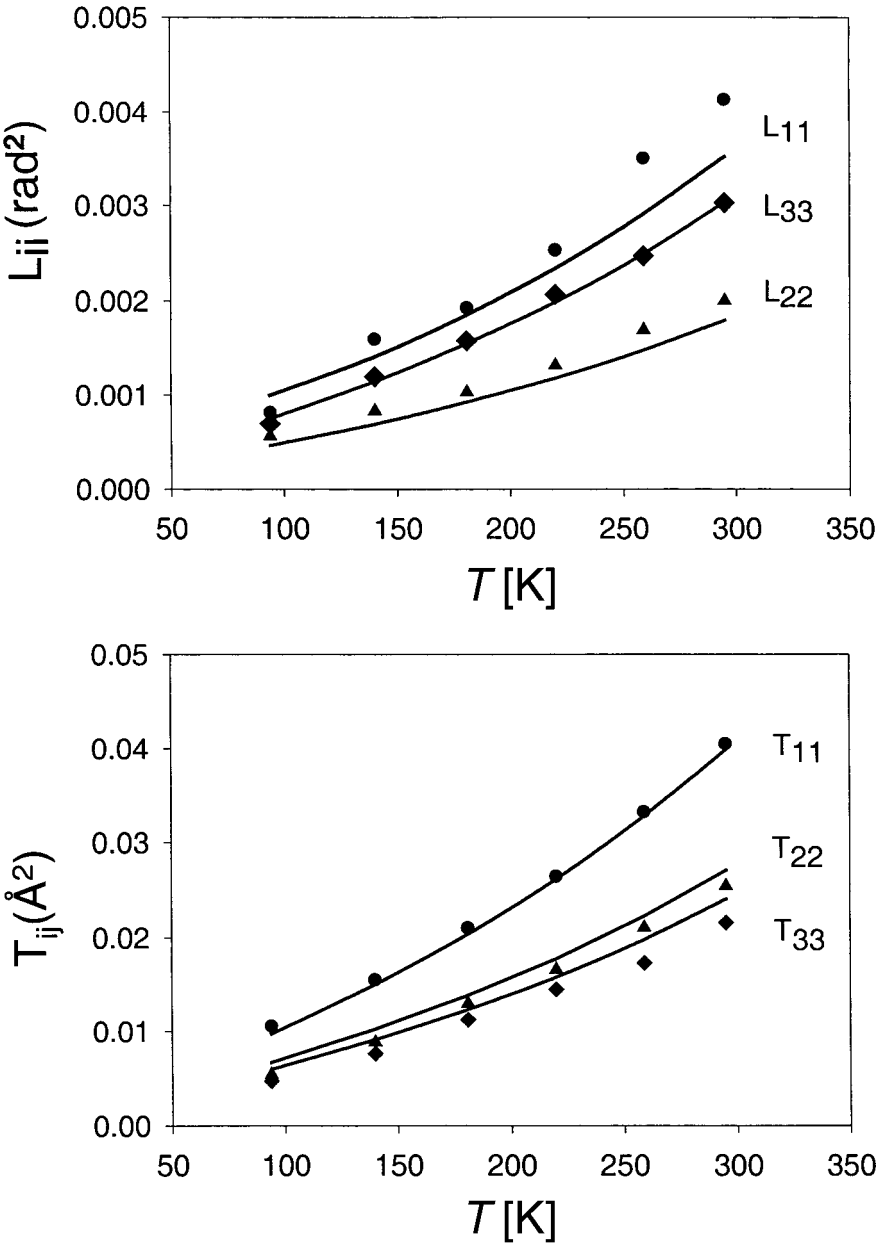

Fig. 3. *Diagonal components of the molecular* **L** *and* **T** *tensors of anthracene, referred to molecular inertial axes*; *values at individual temperatures from rigid-body analysis after correction for internal motion* [10]; *continuous curves from* Einstein *model RB*, b_{1u}, a_u (ε_{all})

deformations of the molecules in their mean crystal field, *2*) atomic $\boldsymbol{\varepsilon}$ tensors accounting for high-frequency molecular vibrations, and *3*) a residual ($\boldsymbol{\varepsilon}_{all}$) accounting for other, largely undefined factors contributing to ADPs. By and large, the questions asked in the introduction may be answered as follows: *1*) the local normal modes account well for the observed temperature dependence of the ADPs. *2*) A rigid-body model is insufficient to reproduce the observed ADPs. Intramolecular amplitudes with varying degrees of temperature dependence are important. Some out-of-plane deformations of anthracene contribute appreciably to the temperature dependence of the ADPs, because their frequencies are in the same range as those of the librational and translational modes. The analogous modes of naphthalene are less important in this respect because their frequencies are significantly higher. *3*) A *Grüneisen* constant takes into account crystal expansion and concomitant weakening of the crystal field with increasing temperature. *4*) High-frequency amplitudes can be extracted directly from neutron and X-ray diffraction ADPs provided the latter have been obtained from multipole refinements. The diffraction results agree with those from normal-mode calculations performed on isolated molecules by density-functional theory. *5*) The residuals $\boldsymbol{\varepsilon}_{all}$ not related to motion, although generally small compared to the ADPs themselves (*ca.* 0.001 A^2 *vs. ca.* 0.01 – 0.1 A^2), are a statistically significant part of the model.

Limitations of this Study. There are two main ones. The first derives from the limited temperature ranges for which X-ray-diffraction data are available (anthracene: 94 – 295 K; naphthalene: 92 – 239 K). The lack of data in the very-low-temperature regime (*ca.* 20 K) prevents the sampling of ADPs in the zero-point-motion regime. This is a significant disadvantage because it makes the determination of the phases of atomic displacements difficult [11]. The very-low-temperature data for the deuterated compounds ((D_{10})anthracene: 16 K; (D_8)naphthalene: 12 K) should compensate for this shortcoming, at least in principle, because the models of motion of different isotopomers are related through the usual condition, equality of the force constants:

$$\begin{aligned}\boldsymbol{F} &= \boldsymbol{g}_H^{-1}\ \boldsymbol{V}_H^{-1}\ \boldsymbol{\lambda}_H\ (\boldsymbol{g}_H^T\ \boldsymbol{V}_H^T)^{-1} \\ &= \boldsymbol{g}_D^{-1}\ \boldsymbol{V}_D^{-1}\ \boldsymbol{\lambda}_D\ (\boldsymbol{g}_D^T\ \boldsymbol{V}_D^T)^{-1}\end{aligned} \tag{3}$$

The matrix $\boldsymbol{\lambda}$ is diagonal with elements ω_i^2. It is another limitation of this work that the present version of the least-squares program NKA for analyzing the temperature evolution of ADPs does not yet provide for the simultaneous analysis of ADPs from different isotopic species [12][13].

Finally, one might ask whether we now know '*the true values of the ADPs*' [10]? The answer is probably '*Not yet*'. An optimistic '*but…*' seems justified, however, because the molecular *Einstein* model used here represents not only a relatively simple scheme for combining ADPs obtained at different temperatures, with different radiation and for different isotopes into an integrated whole that is more than the sum of its parts, but also a rational framework for analyzing their temperature dependence and dissecting them into contributions from different types of motion and from other factors. The former can be checked against independent experimental information, whereas the latter become quantifiable and thus more easily amenable to analysis.

Towards Dynamic Structure Determination? The case study presented here shows how to extract dynamic information from multitemperature ADPs. The reliability of

Table 8. *Results of Anisotropic Refinement of the Neutron-Diffraction Data of (D_8)Naphthalene at 295 K* [22]

	x	y	z	U_{eq}		
C(1)	0.0856(4)	0.0170(6)	0.3257(5)	0.0639(11)		
C(2)	0.1148(3)	0.1595(5)	0.2197(4)	0.0535(10)		
C(3)	0.0483(3)	0.1030(4)	0.0358(4)	0.0409(8)		
C(4)	0.0760(4)	0.2472(6)	−0.0774(5)	0.0496(10)		
C(5)	0.0100(5)	0.1875(6)	−0.2550(5)	0.0602(10)		
D(1)	0.1368(8)	0.0640(11)	0.4657(7)	0.0995(19)		
D(2)	0.1882(6)	0.3169(7)	0.2725(7)	0.0837(16)		
D(4)	0.1502(6)	0.4041(6)	−0.0222(7)	0.0758(15)		
D(5)	0.0340(7)	0.2988(10)	−0.3393(8)	0.0948(18)		
	U_{11}	U_{22}	U_{33}	U_{23}	U_{13}	U_{12}
C(1)	0.064(2)	0.071(3)	0.051(2)	−0.0014(19)	0.0274(19)	0.015(19)
C(2)	0.0512(18)	0.0471(16)	0.0539(19)	−0.0124(16)	0.0232(17)	−0.0062(14)
C(3)	0.0348(15)	0.0321(13)	0.0511(18)	−0.0040(11)	0.0202(13)	−0.0021(10)
C(4)	0.050(2)	0.0378(12)	0.065(2)	0.0023(13)	0.0340(18)	−0.0028(11)
C(5)	0.063(2)	0.0607(19)	0.069(3)	0.013(2)	0.044(2)	0.0051(18)
D(1)	0.113(4)	0.115(4)	0.063(3)	−0.006(3)	0.042(3)	−0.002(4)
D(2)	0.088(3)	0.064(2)	0.079(3)	−0.027(3)	0.033(3)	−0.021(2)
D(4)	0.081(3)	0.0463(18)	0.102(3)	−0.001(2)	0.051(3)	−0.017(2)
D(5)	0.111(4)	0.098(4)	0.099(4)	0.028(3)	0.072(3)	−0.001(3)

such information depends on the quality of the ADPs and, thus, of the diffraction data: they should cover the lowest and the highest temperatures accessible experimentally (*i.e.*, the zero-point-motion and classical regimes); their resolution should be as high as possible at all temperatures. Factors affecting ADPs but not representing motion should be minimized, *e.g.*, through multipole refinement of X-ray data, corrections for thermal diffuse scattering, and careful consideration of absorption, extinction and scan truncation problems. Although it is unlikely – and probably unnecessary – that such studies will ever be done on a routine basis, it should still be pointed out that thanks to the advent of fast area detectors and the availability of intense synchrotron radiation the investments necessary for dynamic structure determination are no longer prohibitive.

We thank Prof. *C. P. Brock* for providing unpublished material

REFERENCES

[1] M. N. Burnett, C. K. Johnson, ORTEP-III, Oak Ridge Thermal Ellipsoid Plotting Program for Crystal Structure Illustrations, ORNL-6895, Oak Ridge National Laboratory, 1996.
[2] W. Hummel, J. Hauser, H. B. Bürgi, *J. Mol. Graphics 8* **1990**, 214.
[3] D. W. J. Cruickshank, *Acta Crystallogr.* **1956**, *9*, 915.
[4] D. W. J. Cruickshank, *Acta Crystallogr.* **1956**, *9*, 754.
[5] V. Schomaker, K. N. Trueblood, *Acta Crystallogr. Sect. B* **1968**, *24*, 63.
[6] C. K. Johnson, in 'Thermal Neutron Diffraction', Ed. B. T. M. Willis, Oxford University Press, London 1970, p. 132.
[7] D. W. J. Cruickshank, *Acta Crystallogr.* **1956**, *9*, 1005.
[8] C. P. Brock, J. D. Dunitz, *Acta Crystallogr. Sect. B* **1990**, *46*, 795.
[9] C. P. Brock, J. D. Dunitz, *Acta Crystallogr. Sect. B* **1982**, *38*, 2218.

[10] C. P. Brock, J. D. Dunitz, F. L. Hirshfeld, *Acta Crystallogr. Sect. B* **1991**, *47*, 789.
[11] H. B. Bürgi, S. C. Capelli, *Acta Crystallogr. Sect. A* **2000**, *56*, 403.
[12] M. Förtsch, Ph.D. Thesis, Universität Bern, 1997.
[13] S. C. Capelli, Ph.D. Thesis, University of Bern, 1999.
[14] S. C. Capelli, M. Förtsch, H. B. Bürgi, *Acta Crystallogr. Sect. A* **2000**, *56*, 413.
[15] H. B. Bürgi, S. C. Capelli, H. Birkedal, *Acta Crystallogr. Sect. A* **2000**, *56*, 425.
[16] E. Grüneisen, in 'Handbuch der Physik', Ed. H. G. K. Scheel, Vol. 10, Springer, Berlin 1926, p. 1.
[17] A. Einstein, *Ann. Phys.* **1907**, *22*, 108.
[18] H. B. Bürgi, M. Förtsch, *J. Mol. Struct*. **1999**, *485–486*, 457.
[19] S. L. Chaplot, N. Lehner, G. S. Pawley, *Acta Crystallogr. Sect. B* **1982**, *38*, 483.
[20] M. S. Lehmann, G. S. Pawley, *Acta Chem. Scand.* **1972**, *26*, 1996
[21] I. Natkaniec, A. V. Belushkin, W. Dyck, H. Fuess, C. M. E. Zeyen, *Z. Kristallogr*. **1983**, *163*, 285.
[22] G. S. Pawley, E. A. Yeats, *Acta Crystallogr. Sect. B* **1969**, *25*, 2009.
[23] X.-D. Gong, H.-M. Xiao, *J. Phys. Org. Chem.* **1999**, *12*, 441.
[24] E. Cané, A. Miani, P. Palmieri, R. Tarroni, A. Trombetti, *J. Chem. Phys.* **1997**, *106*, 9004.
[25] P. Swiderick, G. Hohlneicher, *J. Chem. Phys.* **1993**, *98*, 974.
[26] A. Bree, R. A. Kydd, *J. Chem. Phys.* **1968**, *48*, 5319.
[27] J. G. Radziszewki, J. Michl, *J. Chem. Phys.* **1985**, *82*, 1985.
[28] B. Rousseau, S. T. Maes, A. T. H. Lenstra, *Acta Crystallogr., Sect. A* **2000**, *56*, 300.
[29] F. L. Hirshfeld, *Acta Crystollgr. Sect. A* **1976**, *32*, 239.

Received May 21, 2001